M Rajanna, Pramod; Luchkin, Sergey; Larionov, Konstantin V.; Grebenko, Artem; Popov, Zakhar I.; Sorokin, Pavel B.; Danilson, Mati; Bereznev, Sergei; Lund, Peter D.; Nasibulin, Albert G.

Adhesion of Single-Walled Carbon Nanotube Thin Films with Different Materials

Published in:
Journal of Physical Chemistry Letters

DOI:
10.1021/acs.jpclett.9b03552

Published: 16/01/2020

Document Version
Peer-reviewed accepted author manuscript, also known as Final accepted manuscript or Post-print

Surfaces, Interfaces, and Catalysis; Physical Properties of Nanomaterials and Materials

Adhesion of Single-walled Carbon Nanotube Thin Films with Different Materials

Pramod Mulbagal Rajanna, Sergey Yurevich Luchkin, Konstantin V Larionov, Artem Grebenko, Zakhar I. Popov, Pavel B. Sorokin, Mati Danilson, Sergei Bereznev, Peter D. Lund, and Albert G. Nasibulin

J. Phys. Chem. Lett., **Just Accepted Manuscript** • DOI: 10.1021/acs.jpclett.9b03552 • Publication Date (Web): 31 Dec 2019

Adhesion of Single-walled Carbon Nanotube Thin Films with Different Materials

Pramod M. Rajanna[1,2], Sergey Luchkin[1], Konstantin V. Larionov[3,4,5], Artem Grebenko[1,5], Zakhar I. Popov[3,6], Pavel B. Sorokin[3,4,5], Mati Danilson[7], Sergei Bereznev[7], Peter D. Lund[2], Albert G. Nasibulin[1,2*]*

[1] Skolkovo Institute of Science and Technology, Nobel Street 3, Moscow 121205, Russia

[2] Aalto University, P.O. Box 15100, FI-00076 Aalto, Espoo, Finland

[3] National University of Science and Technology MISIS, 4 Leninskiy Prospekt, Moscow 119049, Russia

[4] Technological Institute for Superhard and Novel Carbon Materials, 7a Centralnaya Street, Troitsk, Moscow 108840, Russia

[5] Moscow Institute of Physics and Technology, Institute Lane 9, Dolgoprudniy, Moscow District, Russia

[6] Emanuel Institute of Biochemical Physics RAS, 4 Kosygina st., Moscow 119334, Russia

[7] Tallinn University of Technology, Department of Materials and Environmental Technology, Ehitajate tee 5, 19086 Tallinn, Estonia

---

*Corresponding authors:

Pramod M. Rajanna,
e-mail: pramod.rajanna@skolkovotech.ru
Albert G. Nasibulin,
e-mail: a.nasibulin@skoltech.ru

Abstract

Single-walled carbon nanotubes (SWCNTs) possess extraordinary physical and chemical properties. Thin films of randomly oriented SWCNTs have great potential in many opto-electro-mechanical applications. However, good adhesion of SWCNT films with a substrate material is pivotal for their practical use. Here, for the first time we systematically investigate the adhesion properties of SWCNT thin films with commonly used substrates such as glass (SiO_2), indium tin oxide (ITO), crystalline silicon (C-Si), amorphous silicon (a-Si:H), zirconium oxide (ZrO_2), platinum (Pt), polydimethylsiloxane (PDMS), and SWCNTs for self-adhesion using atomic force microscopy. By comparing the results obtained in air and inert Ar atmospheres we observed a great contribution of the surface state of the materials on their adhesion properties. We found that the SWCNT thin films have higher adhesion in an inert atmosphere. The adhesion in the air can be greatly improved by a fluorination process. Experimental and theoretical analyses suggest that adhesion depends on the atmospheric conditions and surface functionalization.

TOC GRAPHICS

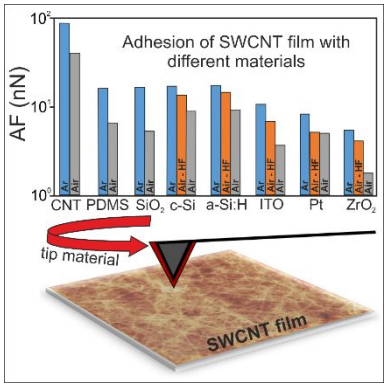

Keywords

Single-walled carbon nanotubes, thin films, adhesion energy, ambient conditions, inert atmosphere, fluorination

The unique properties of single-walled carbon nanotubes (SWCNTs) are attracting extensive interest from the scientific community for different applications[1–7]. The usage of SWCNT networks as efficient transparent conductors is a particular challenge in terms of obtaining conformal films with smooth surfaces as well as creating a firm contact between the film and other materials[8]. The substrate material considerably influences the adhesion of the SWCNT films. The performance of many SWCNT applications is governed by Van der Waals (VdW) interactions with the substrate[9–11], in particular when nanotubes are used as transparent electrodes in opto-electronic devices[8]. The contact between the nanotube film and substrate material impact the interface properties that affects the device efficiency[12,13]. In a SWCNT network, many nanotubes overlap and are suspended over each other without getting in contact with the substrate material, for example in SWCNT/Si solar cell devices decreasing their performance[14,15]. To overcome this, novel approaches have been proposed such as densification of SWCNTs[15–17], acid doping[16–18], and impregnating SWCNTs with conductive polymers[19,20]. Thus, better understanding of the adhesion of nanotube films and the associated mechanisms are important for long-term reliability of devices employing the SWCNT films[21,22].

The significance of the SWCNT adhesion has been discussed[10,23–25] through lateral atomic force microscope (AFM)[9,22,23,26,27], tapping mode AFM[24], dynamic force AFM[25], and theoretical works using continuum analysis and atomistic simulations[11,28,29] probing the adhesive properties of SWCNTs with other materials and between nanotubes themselves[11,21,22,26,27,29–31]. Reported methods have been deduced using either a hypothesis for the interaction of SWCNTs with its environment[11,29] or experimental quantification of multiwalled carbon nanotubes or individual nanotube loop adhesion energy[22,26,27]. However, the experience from SWCNT thin film

applications clearly indicates that the interaction of SWCNT films with the substrate is still an open question.

Here, we quantitatively evaluate the interaction of SWCNT thin films with various commonly used substrate materials (henceforth called materials) using atomic force microscopy (AFM) in air and inert Ar atmospheres. The materials chosen include glass (SiO_2), indium tin oxide (ITO), crystalline silicon (C-Si), amorphous silicon (a-Si:H), zirconium oxide (ZrO_2), platinum (Pt), polydimethylsiloxane (PDMS), and SWCNTs for self-adhesion measurements. We show that the adhesion of randomly oriented SWCNT thin films is strongly influenced by the atmospheric conditions and surface functionalization of the material. The measurements demonstrate higher adhesion in inert atmosphere, but adhesion in air can be greatly improved by a simple fluorination process.

We utilized aerosol synthesized SWCNTs[32,33], which are dry-transferred from a nitrocellulose filter[34] to a desired substrate, which is a Si wafer in this case. Figure S1a in supporting information (SI) shows the cross-sectional SEM image of the SWCNT thin film on the Si wafer and surface of randomly oriented closely connected individual and bundled nanotubes. The thickness of the film was about 44 nm by SEM as shown in Figure S1a and verified from the absorbance spectrum Figure S1b as described by Mikheev *et al.*[35]. This film was investigated in an atomic force microscope by collecting force-distance (F-D) curves between the SWCNT thin film sample and cantilevers coated by a given material as shown in Figure 1.

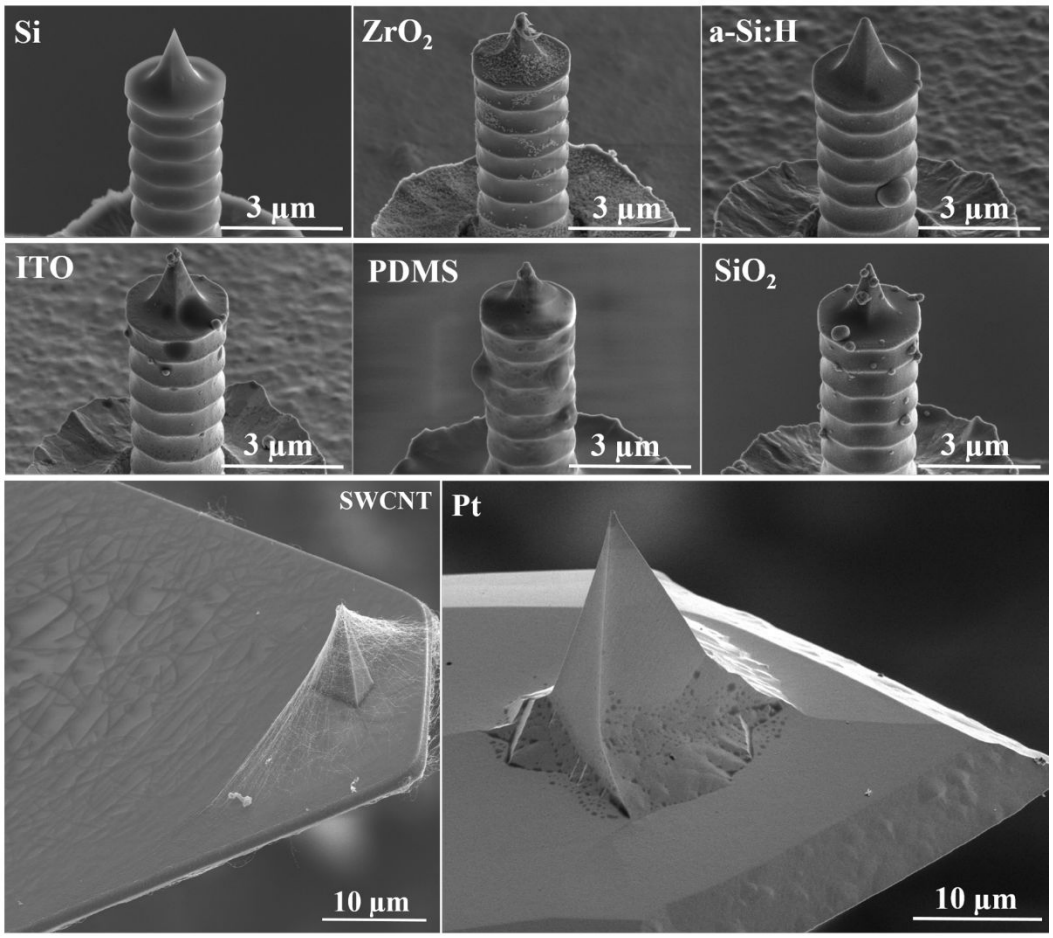

Figure 1. Cantilever tips covered with different materials: Si, ZrO_2, a-Si:H, ITO, PDMS, SiO_2, SWCNT, and Pt.

A flexible lever of the AFM cantilever is clamped from one side on a Si chip installed in a cantilever holder. The other free-standing side with a sharp tip is brought to several tens of nm above the sample surface. Upon the approach, the distance between the tip and the sample is reduced, the tip touches the sample and sets a compressive force on it, which value is determined from the lever upward bending using Hooke's law, $F = k\Delta d$, where k is the cantilever spring constant, and Δd is the distance from onset of the compressive force to the setpoint. After reaching a predefined setpoint force, the tip is retracted from the sample and detach from it at an attractive force (downward lever bending), which is a measure of the adhesion force[36–38]. This force depends

on the experimental conditions such as the maximum force load and the cantilever tip radius. Collected maps of F-D curves (averaged over 65, 536 measurements in air and 1024 measurements in inert Ar atmosphere, as detailed in SI section S1) were analyzed by the microscope software. The sample deformation, adhesion force, and peak force values are extracted from F-D curves[38] as shown in Figure S2. Peak force, or maximum force load, is a predefined set point parameter that is controlled by a microscope feedback loop system.

In order to determine and compare intrinsic adhesion parameters between SWCNTs and a given material, the measured adhesion force must be normalized by the tip-CNT contact area, which is governed by aforementioned force load and tip radius. We used the Hertz model[39] to estimate the tip-surface contact area at the extremum applied force as $S = \pi \times R_{tip} \times h$, where R_{tip} is the tip apex radius and h is the deformation. Within this model we assumed that the tip apex is a rigid sphere of a certain radius R_{tip}, which was measured on the dimpled aluminum substrate[40] (Table S1), the CNT surface is elastic half space, and the strain is in the elastic limit. We neglected surface roughness as well. Despite the fact that in the Hertz model the contact is nonadhesive, it can be accurately applied to adhesive contacts when the adhesive force is small as compared to the applied force. The maximum applied force is limited due to the fact that the probe is likely to drop through a meshy SWCNT surface upon high force loading. As a result, the tip-sample contact area sharply increased due to side contacts of the tip with surrounding CNTs, leading to the boost of the adhesion force (e.g. Figure 2a and 2b shows the change in the slope of adhesion force with deformation for ZrO_2 at a peak force of 50 nN as in the inset). With this assumption we attribute the moment of the tip drop with the slope break in the plots shown in Figure 2a and 2b, respectively. With increasing applied force, the adhesion force demonstrates a gradual linear growth. Applying the force of 50 nN resulted in a steep gain of the adhesion force and in some cases cutback of the

deformation as shown in Figure 2b and corresponding F-D curves in Figure S2. The plots for other materials are available in Figure S3. For all the materials the slope break happened after 50 nN applied force, so we used this value for the Hertz model. The measured adhesion force (AF) as described above[36–38] and the calculated surface adhesion force density (SAFD), which is the adhesion force normalized to the contact area, are represented in Figure 3 and Figure S4.

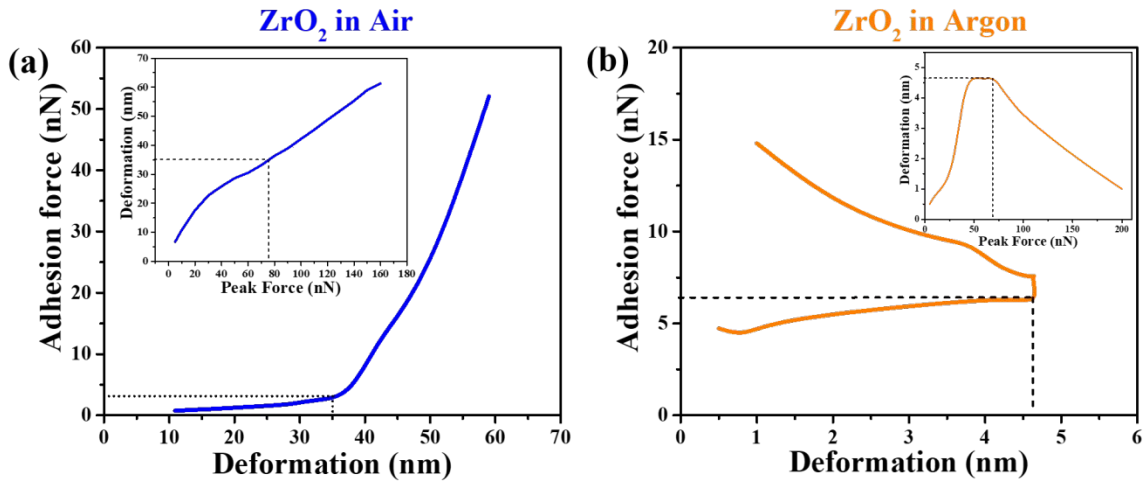

Figure 2. Adhesion force *versus* deformation measured in **(a)** air and **(b)** inert Ar atmospheres between SWCNT film and ZrO_2.

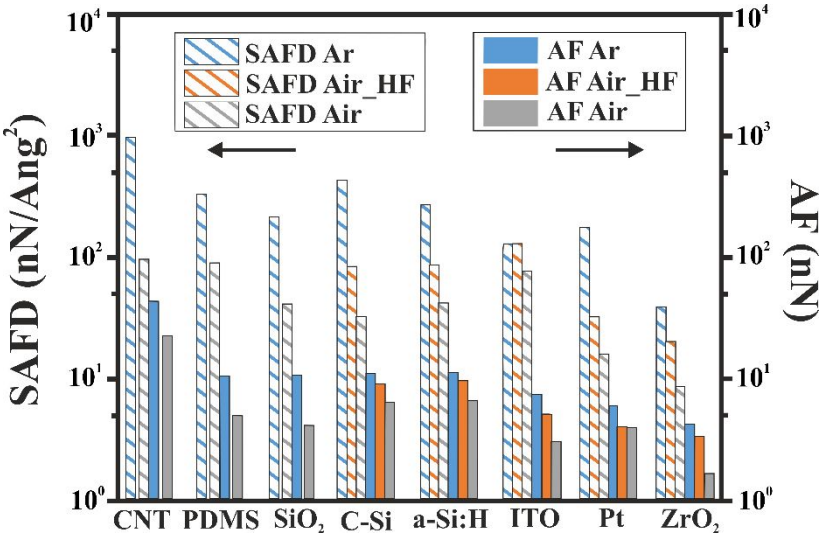

Figure 3. Adhesion force (AF) (right axis, solid bars) and surface adhesion force density (SAFD) (left axis, dashed bars) of SWCNT thin films with various materials.

For all studied materials, the normalized adhesion force (adhesion force density) in the inert Ar atmosphere is higher than in ambient air, which can be explained by the difference in the ambient humidity and its influence on the SWCNTs as shown by Shandakov *et al.*[41]. The relative humidity (RH) can affect adhesive properties, especially in nanoscale, due to formation of a capillary bridge when RH exceeds roughly a threshold value of 25%[42–44]. The capillary force strongly depends on the sample local curvature, which affects the capillary bridge geometry resulting in higher adhesion force for concave surface and smaller adhesion force for convex surface[42,45]. On hydrophilic surfaces, increasing humidity results in increasing the pull-off force, whereas on hydrophobic surfaces humidity has negligible effect[46,47]. Since SWCNTs are hydrophobic[48] and possess convex surface geometry, the capillary bridge effect is likely to be negligible. Instead, the smaller adhesion force in air is better explained by the reduction of the VdW forces in a polar water medium between the tip and the SWCNT thin film[28,49] (SI Section S3.1 Discussion).

The experimentally measured adhesion force shown in Figure 3 can explain the following observations: SWCNTs thin film are easily dry-transferred onto a-Si:H, Si, SiO_2, and PDMS in air, while under the same conditions the transfer onto ITO and Pt is complicated and completely failed on ZrO_2. However, the same SWCNT thin films are easily dry-transferred on all the materials in an inert atmosphere.

To verify that the adhesion force is strongly dependent on the humidity, we fluorinated the a-Si:H, C-Si, ZrO_2, ITO, and Pt coated tips. The process of fluorination is well-known to alter the surface properties of materials without changing the bulk characteristics of the pristine

material[50,51]. The altered properties may concern wettability, adhesion, chemical stability, permeation, electrical conductivity, bio-compatibility, grafting, mechanical behavior, and several others[50]. We used the dry process fluorination, which proceeds spontaneously at room temperature by exposing the samples to hydrofluoric (HF) vapor for 60 seconds. Each tip was calibrated once again immediately after the HF treatment and the adhesion force measurements were conducted on the same SWCNTs thin film in air at the peak force of 50 nN. The measured adhesion forces were recorded for the HF treated tips and shown in Figure 3 showing that the adhesion force increased for all HF treated tips. This trend is similar to the adhesion force measurements conducted in the inert atmosphere. Moreover, after the fluorination process SWCNT films can be easily dry-transferred even on the problematic materials, such as ITO, Pt, and ZrO_2.

To understand the role of fluorination in improving the adhesion of SWCNT thin films and its chemical composition, X-ray photoelectron spectroscopy (XPS) was carried out on ZrO_2 and a-Si:H tips (SI section S4). The XPS infers that fluorinating the surface of the material in air modifies the chemical composition by partially eliminating the presence of humidity and creating fluorine terminated Zr and C bonds (Figure S5 d, e, f, g, and h), which aides in improved adhesion and explains the easy dry-transfer of SWCNTs on ZrO_2 after HF treatment at ambient conditions.

The experimental measurements were realized in three different conditions using atomic force microscopy: ambient air, HF treatment in air, and inert Ar atmosphere. Ambient air leads to material surface contamination and the use of HF treatment in air helps to partially clean it by elimination of the native oxides and water vapor as was demonstrated in a number of experimental and theoretical works[52–54].

In order to explain the dependence of SWCNT thin film adhesion on the different materials and environmental conditions, we carry out density functional theory (DFT) (described in SI

section S5). In compliance with our experimental conditions, three different cases with Si, Pt, ITO, and SiO_2 materials are studied however replacing SWCNTs with graphene monolayer. Inert atmosphere conditions are realized as the graphene monolayer on the clean material surface, HF treatment in air is simulated as the graphene monolayer on the hydrogenated material surface. In the calculations HF treatment in air is considered as hydrogenated surfaces and not specifically with fluorine atoms as the intention was to analyze the effects of different environmental conditions only. Also, data on fluorinated bonds was too limited for detailed DFT analysis in our case. Finally, ambient air conditions are represented as the graphene monolayer on the material surface passivated by OH or CO groups[52,55,56].

Calculation of the adhesion energy attributed to the VdW interaction was made directly by the following equation:

$$E_{adh}\left(\frac{\mathrm{eV}}{\mathrm{\AA}^2}\right) = \frac{1}{\mathrm{A}}\left(E_{total} - \left(E_C + E_{sub}\right)\right), \qquad (1)$$

where A is the contact area between the graphene and the substrate in the unit cell, E_{total} is the total energy of the graphene/substrate system, E_C and E_{sub} are the energies of separate graphene and substrate, respectively.

A comparison of the calculated adhesion energy (E_{adh}) and experimental adhesion force density (SAFD) for Si, Pt, ITO and SiO_2 under different conditions is shown in Figure 4. Here, theoretical and experimental values are shown by solid bars (left axis) and dashed bars (right axis, logarithmic scale), respectively. By blue (Ar), orange (HF), and grey (Air) colors, we depict the inert atmosphere, HF treatment in air, and ambient air conditions, respectively. Atomic models of pristine interfaces (as in the inert atmosphere) after the DFT optimization are shown below the corresponding material names in Figure 4. For the Si case, optimized atomic models of the

interface passivated by H (HF treatment in air) and OH (ambient air) are shown as well in the dashed box (bottom left). The other atomic models are represented in Figure S6.

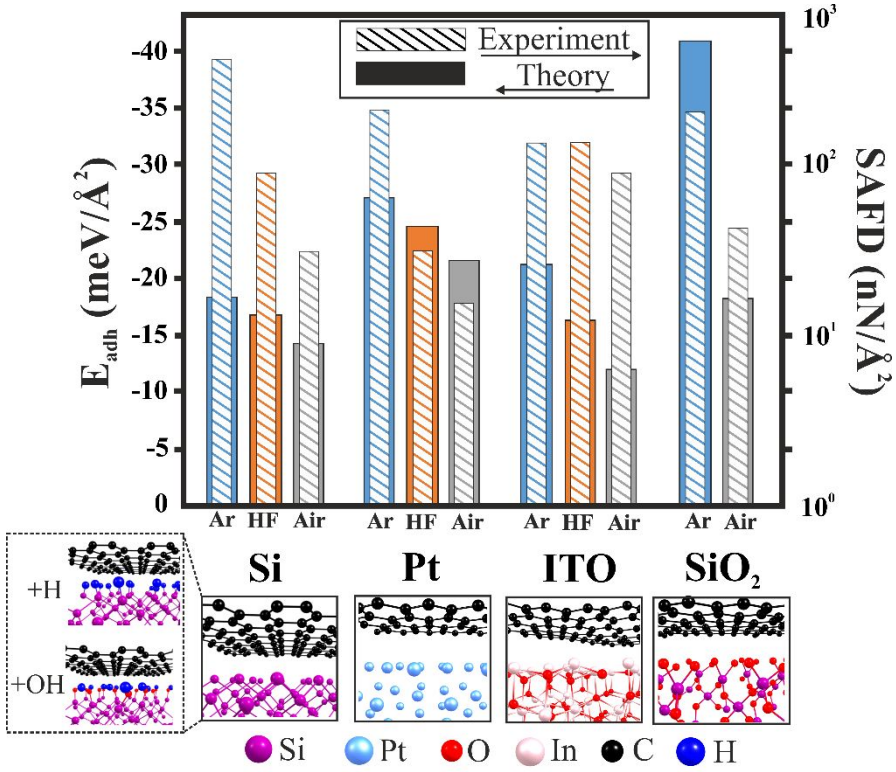

Figure 4. Comparison of the calculated adhesion energy (left axis, solid bars) and experimental adhesion force density (right axis, dashed bars) for Si, Pt, ITO and SiO_2 under different environmental conditions, where Ar corresponds to the inert atmosphere, HF stands for HF treatment in air, and Air is the air condition. Atomic models of pristine interfaces (as in the inert atmosphere) and Si surface functionalized by H or OH groups are shown as an example below the corresponding graphs. The other atomic models are shown in Figure S6.

From Figure 4, we see a good correspondence between the experimental measurements and DFT simulations yielding the main effect of adhesion change under different conditions. Indeed, for every case of the graphene-material model, the pristine surface (blue solid bars) have higher adhesion energies than for the hydrogenated surfaces (orange solid bars). Also, the hydrogenated

surfaces have stronger interaction with graphene than in the case of their passivation by OH or CO groups (grey solid bars). The same monotonous trends are observed for the experimentally measured SAFD values shown in the logarithmic scale for a better representation (dashed bars).

From the DFT simulations, we can conclude that contaminated material surface in ambient air worsen the adhesion with graphene (carbon nanotubes). But, through preliminary HF treatment of the material surface, native oxides and water vapors are possibly partially eliminated that results in improved adhesion for graphene (carbon nanotubes). At the same time, the inert atmosphere conditions allow to additionally get rid of any intermediate functional groups on the surface of the material and approach to almost direct interaction of the partially clean SWCNT and AFM tip as demonstrated in the real experiment.

In summary, for the first time we carried out adhesion force measurements of randomly oriented SWCNT thin films in air and inert atmospheres with various materials deposited directly on the AFM tips. Quantitative values were derived for the adhesion force from the force-distance curves by estimating the tip-surface contact area according to the Hertz model. Through experimental observations and theoretical simulations, we conclude that the adhesion is greatly influenced by the environmental conditions and the surface functionalization. We observe that the SWCNT thin films have better adhesion in an inert atmosphere. The adhesion affected by storing the samples in the ambient air conditions can be greatly improved by a simple fluorination process. The present work provides new insight to the physical mechanisms of SWCNT thin film adhesion that will succeed in its efficient usage with its exceptional properties for future roll-to-roll applications.

ASSOCIATED CONTENT

Supporting Information.

Methods (S1), SWCNT film characterization (S2), AFM measurements (S3), Discussion (S3.1), XPS of ZrO_2 and a-Si:H cantilever tips (S4), Theoretical Simulation of adhesion energy (S5).

AUTHOR INFORMATION

Corresponding authors:

e-mail: pramod.rajanna@skolkovotech.ru

e-mail: a.nasibulin@skoltech.ru

ACKNOWLEDGEMENT

Authors thank Ivan S. Mukhin of Saint Petersburg Academic University and ITMO University for a-Si:H and ITO depositions. Authors thank Aapo Poskela, Aalto University for ZrO_2 deposition and Dr. Lide Yao, Aalto University for SEM measurements of SWCNT thin film cross-section and morphology. P.M.R. and A.G.N. acknowledge the Russian Science Foundation for the support (synthesis of SWCNTs) by project # 17-19-01787. K.V.L., Z.I.P. and P.B.S. gratefully acknowledge the financial support of the Ministry of Education and Science of the Russian Federation in the framework of Increase Competitiveness Program of NUST "MISiS" (No. K2-2019-016). K.V.L. and P.B.S. gratefully acknowledge Grant of President of Russian Federation for government support of young DSc. (MD-1046.2019.2). The authors are grateful to supercomputer cluster NUST "MISiS" provided by Materials Modeling and Development Laboratory (supported via the Grant from the Ministry of Education and Science of the Russian Federation No. 14.Y26.31.0005) and to the Joint Supercomputer Center of the Russian Academy of Sciences. M.D. and S.B. acknowledge the support by institutional research funding IUT19-28 of the Estonian Ministry of Education and the European Union through the European Regional

Development Fund, Project TK141. P.M.R thanks for the partial financial support from EDUFI Fellowship (# TM-19-11028) from Finnish National Agency for Education.

REFERENCES

(1) Jariwala, D.; Sangwan, V. K.; Lauhon, L. J.; Marks, T. J.; Hersam, M. C. Carbon Nanomaterials for Electronics, Optoelectronics, Photovoltaics, and Sensing. *Chemical Society Reviews*. 2013. https://doi.org/10.1039/c2cs35335k.

(2) Tian, Y.; Timmermans, M. Y.; Kivistö, S.; Nasibulin, A. G.; Zhu, Z.; Jiang, H.; Okhotnikov, O. G.; Kauppinen, E. I. Tailoring the Diameter of Single-Walled Carbon Nanotubes for Optical Applications. *Nano Res.* **2011**. https://doi.org/10.1007/s12274-011-0137-6.

(3) Baughman, R. H.; Zakhidov, A. A.; De Heer, W. A. Carbon Nanotubes - The Route toward Applications. *Science*. 2002.

https://doi.org/10.1126/science.1060928.

(4) Jeon, I.; Matsuo, Y.; Maruyama, S. Single-Walled Carbon Nanotubes in Solar Cells. *Topics in Current Chemistry*. 2018. https://doi.org/10.1007/s41061-017-0181-0.

(5) Avouris, P.; Chen, Z.; Perebeinos, V. Carbon-Based Electronics. *Nature Nanotechnology*. 2007. https://doi.org/10.1038/nnano.2007.300.

(6) Liu, Y.; Wang, F.; Wang, X.; Wang, X.; Flahaut, E.; Liu, X.; Li, Y.; Wang, X.; Xu, Y.; Shi, Y.; et al. Planar Carbon Nanotube-Graphene Hybrid Films for High-Performance Broadband Photodetectors. *Nat. Commun.* **2015**, *6*, 1–7. https://doi.org/10.1038/ncomms9589.

(7) Sun, D. M.; Timmermans, M. Y.; Tian, Y.; Nasibulin, A. G.; Kauppinen, E. I.; Kishimoto, S.; Mizutani, T.; Ohno, Y. Flexible High-Performance Carbon Nanotube Integrated Circuits. *Nat. Nanotechnol.* **2011**. https://doi.org/10.1038/nnano.2011.1.

(8) Ellmer, K. Past Achievements and Future Challenges in the Development of Optically Transparent Electrodes. *Nature Photonics*. 2012. https://doi.org/10.1038/nphoton.2012.282.

(9) Hertel, T.; Walkup, R. E.; Avouris, P. Deformation of Carbon Nanotubes by Surface van Der Waals Forces. *Phys. Rev. B - Condens. Matter Mater. Phys.* **1998**. https://doi.org/10.1103/PhysRevB.58.13870.

(10) Hertel, T.; Martel, R.; Avouris, P. Manipulation of Individual Carbon Nanotubes and Their Interaction with Surfaces. *J. Phys. Chem. B* **2002**. https://doi.org/10.1021/jp9734686.

(11) Tang, T.; Jagota, A.; Hui, C. Y. Adhesion between Single-Walled Carbon

Nanotubes. *J. Appl. Phys.* **2005**, *97* (7). https://doi.org/10.1063/1.1871358.

(12) Li, X.; Jung, Y.; Sakimoto, K.; Goh, T. H.; Reed, M. A.; Taylor, A. D. Improved Efficiency of Smooth and Aligned Single Walled Carbon Nanotube/Silicon Hybrid Solar Cells. *Energy Environ. Sci.* **2013**. https://doi.org/10.1039/c2ee23716d.

(13) Rajanna, P. M.; Meddeb, H.; Sergeev, O.; Tsapenko, A. P.; Bereznev, S.; Vehse, M.; Volobujeva, O.; Danilson, M.; Lund, P. D.; Nasibulin, A. G. Rational Design of Highly Efficient Flexible and Transparent P-Type Composite Electrode Based on Single-Walled Carbon Nanotubes. *Nano Energy* **2019**. https://doi.org/10.1016/j.nanoen.2019.104183.

(14) Jia, Y.; Wei, J.; Wang, K.; Cao, A.; Shu, Q.; Gui, X.; Zhu, Y.; Zhuang, D.; Zhang, G.; Ma, B.; et al. Nanotube-Silicon Heterojunction Solar Cells. *Adv. Mater.* **2008**, *20* (23), 4594–4598. https://doi.org/10.1002/adma.200801810.

(15) Hu, X.; Hou, P.; Liu, C.; Cheng, H. Carbon Nanotube/Silicon Heterojunctions for Photovoltaic Applications. *Nano Mater. Sci.* **2019**, No. March, 1–17. https://doi.org/10.1016/j.nanoms.2019.03.001.

(16) Azoubel, S.; Magdassi, S. Controlling Adhesion Properties of SWCNT-PET Films Prepared by Wet Deposition. *ACS Appl. Mater. Interfaces* **2014**. https://doi.org/10.1021/am501488p.

(17) Santidrián, A.; Sanahuja, O.; Villacampa, B.; Diez, J. L.; Benito, A. M.; Maser, W. K.; Muñoz, E.; Ansón-Casaos, A. Chemical Postdeposition Treatments to Improve the Adhesion of Carbon Nanotube Films on Plastic Substrates. *ACS Omega* **2019**. https://doi.org/10.1021/acsomega.8b03475.

(18) Jia, Y.; Cao, A.; Bai, X.; Li, Z.; Zhang, L.; Guo, N.; Wei, J.; Wang, K.; Zhu,

H.; Wu, D.; et al. Achieving High Efficiency Silicon-Carbon Nanotube Heterojunction Solar Cells by Acid Doping. *Nano Lett.* **2011**. https://doi.org/10.1021/nl2002632.

(19) Rajanna, P. M.; Gilshteyn, E. P.; Yagafarov, T.; Aleekseeva, A. K.; Anisimov, A. S.; Neumüller, A.; Sergeev, O.; Bereznev, S.; Maricheva, J.; Nasibulin, A. G. Enhanced Efficiency of Hybrid Amorphous Silicon Solar Cells Based on Single-Walled Carbon Nanotubes and Polymer Composite Thin Film. *Nanotechnology* **2018**, *29* (10). https://doi.org/10.1088/1361-6528/aaa647.

(20) Fan, Q.; Zhang, Q.; Zhou, W.; Xia, X.; Yang, F.; Zhang, N.; Xiao, S.; Li, K.; Gu, X.; Xiao, Z.; et al. Novel Approach to Enhance Efficiency of Hybrid Silicon-Based Solar Cells via Synergistic Effects of Polymer and Carbon Nanotube Composite Film. *Nano Energy* **2017**. https://doi.org/10.1016/j.nanoen.2017.02.003.

(21) Li, W.; Li, Y.; Sheng, M.; Cui, S.; Wang, Z.; Zhang, X.; Yang, C.; Yu, Z.; Zhang, Y.; Tian, S.; et al. Enhanced Adhesion of Carbon Nanotubes by Dopamine Modification. *Langmuir* **2019**. https://doi.org/10.1021/acs.langmuir.9b00192.

(22) Buchoux, J.; Bellon, L.; Marsaudon, S.; Aimé, J. P. Carbon Nanotubes Adhesion and Nanomechanical Behavior from Peeling Force Spectroscopy. *Eur. Phys. J. B* **2011**. https://doi.org/10.1140/epjb/e2011-20204-1.

(23) Falvo, M. R.; Taylor, R. M.; Helser, A.; Chi, V.; Brooks, F. P.; Washburn, S.; Superfine, R. Nanometre-Scale Rolling and Sliding of Carbon Nanotubes. *Nature* **1999**. https://doi.org/10.1038/16662.

(24) Akita, S.; Nishijima, H.; Nakayama, Y. Influence of Stiffness of Carbon-

Nanotube Probes in Atomic Force Microscopy. *J. Phys. D. Appl. Phys.* **2000**. https://doi.org/10.1088/0022-3727/33/21/301.

(25) Lee, S. W.; Kim, K. K.; Cui, Y.; Lim, S. C.; Cho, Y. W.; Kim, S. M.; Lee, Y. H. Adhesion Test of Carbon Nanotube Film Coated onto Transparent Conducting Substrates. *Nano* **2010**, *5* (3), 133–138. https://doi.org/10.1142/S1793292010002025.

(26) Li, T.; Ayari, A.; Bellon, L. Adhesion Energy of Single Wall Carbon Nanotube Loops on Various Substrates. *J. Appl. Phys.* **2015**. https://doi.org/10.1063/1.4919355.

(27) Whittaker, J. D.; Minot, E. D.; Tanenbaum, D. M.; McEuen, P. L.; Davis, R. C. Measurement of the Adhesion Force between Carbon Nanotubes and a Silicon Dioxide Substrate. *Nano Lett.* **2006**. https://doi.org/10.1021/nl060018t.

(28) Leite, F. L.; Bueno, C. C.; Da Róz, A. L.; Ziemath, E. C.; Oliveira, O. N. Theoretical Models for Surface Forces and Adhesion and Their Measurement Using Atomic Force Microscopy. *International Journal of Molecular Sciences*. 2012. https://doi.org/10.3390/ijms131012773.

(29) Yuan, X.; Wang, Y. Adhesion of Single- and Multi-Walled Carbon Nanotubes to Silicon Substrate: Atomistic Simulations and Continuum Analysis. *J. Phys. D. Appl. Phys.* **2017**, *50* (39). https://doi.org/10.1088/1361-6463/aa81b0.

(30) Hashimoto, A.; Takei, Y.; Iwase, E.; Matsumoto, K.; Shimoyama, I. Adhesion Force Mesurement between Silicon and Carbon Nanotubes Synthesized by Chemical Vapor Deposition. In *TRANSDUCERS 2009 - 15th International Conference on Solid-State Sensors, Actuators and*

Microsystems; 2009. https://doi.org/10.1109/SENSOR.2009.5285641.

(31) Zhao, B.; Qi, H.; Liu, X.; Xu, D. Measurement of Adhesive Force between Single-Walled Carbon Nanotube and Ti. *Fullerenes Nanotub. Carbon Nanostructures* **2012**. https://doi.org/10.1080/1536383X.2011.579667.

(32) Nasibulin, A. G.; Kaskela, A.; Mustonen, K.; Anisimov, A. S.; Ruiz, V.; Kivistö, S.; Rackauskas, S.; Timmermans, M. Y.; Pudas, M.; Aitchison, B.; et al. Multifunctional Free-Standing Single-Walled Carbon Nanotube Films. *ACS Nano* **2011**. https://doi.org/10.1021/nn200338r.

(33) Moisala, A.; Nasibulin, A. G.; Brown, D. P.; Jiang, H.; Khriachtchev, L.; Kauppinen, E. I. Single-Walled Carbon Nanotube Synthesis Using Ferrocene and Iron Pentacarbonyl in a Laminar Flow Reactor. *Chem. Eng. Sci.* **2006**. https://doi.org/10.1016/j.ces.2006.02.020.

(34) Kaskela, A.; Nasibulin, A. G.; Timmermans, M. Y.; Aitchison, B.; Papadimitratos, A.; Tian, Y.; Zhu, Z.; Jiang, H.; Brown, D. P.; Zakhidov, A.; et al. Aerosol-Synthesized SWCNT Networks with Tunable Conductivity and Transparency by a Dry Transfer Technique. *Nano Lett.* **2010**. https://doi.org/10.1021/nl101680s.

(35) Mikheev, G. M.; Nasibulin, A. G.; Zonov, R. G.; Kaskela, A.; Kauppinen, E. I. Photon-Drag Effect in Single-Walled Carbon Nanotube Films. *Nano Lett.* **2012**, *12* (1), 77–83. https://doi.org/10.1021/nl203003p.

(36) Adam Moser, Kevin Range, and D. M. Y. Adhesion Force Measurements Using an Atomic Force Microscope Upgraded with a Linear Position Sensitive Detector. *Bone* **2008**, *23* (1), 1–7. https://doi.org/10.1038/jid.2014.371.

(37) Butt, H. J.; Cappella, B.; Kappl, M. Force Measurements with the Atomic Force Microscope: Technique, Interpretation and Applications. *Surf. Sci. Rep.* **2005**, *59* (1–6), 1–152. https://doi.org/10.1016/j.surfrep.2005.08.003.

(38) Cappella, B.; Baschieri, P.; Frediani, C.; Miccoli, P.; Ascoli, C. Force-Distance Curves by AFM. *IEEE Eng. Med. Biol. Mag.* **1997**, *16* (2), 58–65. https://doi.org/10.1109/51.582177.

(39) Meyer, E.; Gyalog, T.; Overney, R. M.; Dransfeld, K. *Nanoscience: Friction and Rheology on the Nanometer Scale*; 2012. https://doi.org/10.1142/3026.

(40) Dremov, V.; Fedoseev, V.; Fedorov, P.; Grebenko, A. Fast and Reliable Method of Conductive Carbon Nanotube-Probe Fabrication for Scanning Probe Microscopy. *Rev. Sci. Instrum.* **2015**. https://doi.org/10.1063/1.4921323.

(41) Shandakov, S. D.; Lomakin, M. V.; Nasibulin, A. G. The Effect of the Environment on the Electronic Properties of Single-Walled Carbon Nanotubes. *Tech. Phys. Lett.* **2016**. https://doi.org/10.1134/S1063785016110080.

(42) Paajanen, M.; Katainen, J.; Pakarinen, O. H.; Foster, A. S.; Lahtinen, J. Experimental Humidity Dependency of Small Particle Adhesion on Silica and Titania. *J. Colloid Interface Sci.* **2006**. https://doi.org/10.1016/j.jcis.2006.09.017.

(43) Weeks, B. L.; Vaughn, M. W.; Deyoreo, J. J. Direct Imaging of Meniscus Formation in Atomic Force Microscopy Using Environmental Scanning Electron Microscopy. *Langmuir* **2005**. https://doi.org/10.1021/la0512087.

(44) Xiao, X.; Qian, L. Investigation of Humidity-Dependent Capillary Force.

Langmuir **2000**. https://doi.org/10.1021/la000770o.

(45) Sirghi, L.; Nakagiri, N.; Sugisaki, K.; Sugimura, H.; Takai, O. Effect of Sample Topography on Adhesive Force in Atomic Force Spectroscopy Measurements in Air. *Langmuir* **2000**. https://doi.org/10.1021/la000392n.

(46) Jones, R.; Pollock, H. M.; Cleaver, J. A. S.; Hodges, C. S. Adhesion Forces between Glass and Silicon Surfaces in Air Studied by AFM: Effects of Relative Humidity, Particle Size, Roughness, and Surface Treatment. *Langmuir* **2002**. https://doi.org/10.1021/la0259196.

(47) Fukunishi, A.; Mori, Y. Adhesion Force between Particles and Substrate in a Humid Atmosphere Studied by Atomic Force Microscopy. *Adv. Powder Technol.* **2006**. https://doi.org/10.1163/156855206778440552.

(48) Kyakuno, H.; Fukasawa, M.; Ichimura, R.; Matsuda, K.; Nakai, Y.; Miyata, Y.; Saito, T.; Maniwa, Y. Diameter-Dependent Hydrophobicity in Carbon Nanotubes. *J. Chem. Phys.* **2016**. https://doi.org/10.1063/1.4960609.

(49) McLachlan, a. D. Retarded Dispersion Forces in Dielectrics at Finite Temperatures. *Proc. R. Soc. A Math. Phys. Eng. Sci.* **1963**. https://doi.org/10.1098/rspa.1963.0115.

(50) Tressaud, A.; Durand, E.; Labrugère, C.; Kharitonov, A. P.; Kharitonova, L. N. Modification of Surface Properties of Carbon-Based and Polymeric Materials through Fluorination Routes: From Fundamental Research to Industrial Applications. *J. Fluor. Chem.* **2007**. https://doi.org/10.1016/j.jfluchem.2006.12.015.

(51) Liang, T.; Neumann, C. N.; Ritter, T. Introduction of Fluorine and Fluorine-Containing Functional Groups. *Angewandte Chemie - International Edition*.

2013. https://doi.org/10.1002/anie.201206566.

(52) Wu, C. J.; Carter, E. A. Mechanistic Predictions for Fluorine Etching of Si(100). *J. Am. Chem. Soc.* **1991**. https://doi.org/10.1021/ja00024a005.

(53) Kang, J. K.; Musgrave, C. B. The Mechanism of HF/H2O Chemical Etching of SiO2. *J. Chem. Phys.* **2002**, *116* (1), 275–280. https://doi.org/10.1063/1.1420729.

(54) Dhar, S.; Seitz, O.; Halls, M. D.; Choi, S.; Chabal, Y. J.; Feldman, L. C. Chemical Properties of Oxidized Silicon Carbide Surfaces upon Etching in Hydrofluoric Acid. *J. Am. Chem. Soc.* **2009**. https://doi.org/10.1021/ja9053465.

(55) Donley, C.; Dunphy, D.; Paine, D.; Carter, C.; Nebesny, K.; Lee, P.; Alloway, D.; Armstrong, N. R. Characterization of Indium-Tin Oxide Interfaces Using X-Ray Photoelectron Spectroscopy and Redox Processes of a Chemisorbed Probe Molecule: Effect of Surface Pretreatment Conditions. *Langmuir* **2002**. https://doi.org/10.1021/la011101t.

(56) Ertl, G.; Neumann, M.; Streit, K. M. Chemisorption of CO on the Pt(111) Surface. *Surf. Sci.* **1977**. https://doi.org/10.1016/0039-6028(77)90052-8.